# IMTA model online

**Data** · December 2012



**5 authors**, including:

David R Plew
National Institute of Water and Atmospheric Research
**46** PUBLICATIONS **1,014** CITATIONS
SEE PROFILE

Jeffrey S Ren
National Institute of Water and Atmospheric Research
**30** PUBLICATIONS **676** CITATIONS
SEE PROFILE

Jeanie Stenton-Dozey
National Institute of Water and Atmospheric Research
**30** PUBLICATIONS **1,087** CITATIONS
SEE PROFILE

Mark Gall
National Institute of Water and Atmospheric Research
**36** PUBLICATIONS **3,472** CITATIONS
SEE PROFILE

Ecological Modelling 246 (2012) 34–46

Contents lists available at SciVerse ScienceDirect

Ecological Modelling

journal homepage: www.elsevier.com/locate/ecolmodel

# An ecosystem model for optimising production in integrated multitrophic aquaculture systems

Jeffrey S. Ren[a,*], Jeanie Stenton-Dozey[a], David R. Plew[a], Jianguang Fang[b], Mark Gall[a]

[a] National Institute of Water and Atmospheric Research, 10 Kyle Street, P.O. Box 8602, Christchurch 8440, New Zealand
[b] Yellow Sea Fisheries Research Institute, 106 Nanjing Road, Qingdao 266071, People's Republic of China

ARTICLE INFO

*Article history:*
Received 29 March 2012
Received in revised form 10 July 2012
Accepted 12 July 2012

*Keywords:*
Integrated multitrophic aquaculture model
Dynamic energy budget
Biomitigation
Productivity

ABSTRACT

Integrated multitrophic aquaculture (IMTA) aims to be an ecologically balanced aquaculture practice that co-cultures species from multiple trophic levels to optimise the recycling of farm waste as a food resource. It provides an opportunity for product diversification and an increase in economic return if managed at the optimal stocking densities for each co-cultured species. A generic IMTA ecosystem model, incorporating dynamic energy budgets for a number of co-culture species from different trophic levels was developed to design IMTA farms for optimisation of multispecies productivity. It is based on the trophic similarity in the ecophysiological behaviour of cultured organisms to describe the uptake and use of energy. This approach can accommodate different species within a trophic group and is transferable to IMTA operations based on finfish–shellfish-detritivore-primary producer systems. Model simulations were firstly performed considering the monoculture of mussels and finfish, each "farm" interacting with the natural variability of the local environment. The next step was running the IMTA model with the co-culture groups added in: one run was with finfish as the key species in co-culture with seaweed and sea cucumbers and the other with mussels as the key culture species in association with seaweed and sea cucumbers. Scenario simulations show that conversion from monoculture to IMTA would considerably reduce waste products and increase farm productivity. Although the development of IMTA practices will depend on acceptable levels of waste products, feasibility and profitability of culture operations, the IMTA model provides a research tool for designing IMTA practices and to understand species interactions and predict productivity of IMTA farms. The refinement of the model and its power to predict multispecies productivity depends on emerging data from trial and commercial sea-based IMTA operations.



## 1. Introduction

Over the past decade, integrated multitrophic aquaculture (IMTA) has received much attention as a means of practicing sustainable aquaculture by recycling nutrients through co-cultured species from different trophic levels (Chopin et al., 2008). The waste (feed) and by-products (faeces and nutrients) from fed species (e.g. finfish) and filtering feeders (e.g. shellfish) become food for extractive species (e.g. detritivores and seaweed) to reduce farm-derived organic and nutrient loading into the environment. Integrated aquaculture has been practiced for centuries in China, initially through land-based operations which later expanded to include marine systems (NACA, 1989; Yang et al., 2000). Such integrated culture techniques have recently been incorporated into scientific-based experiments which monitor the feeding and growth of a mixture of species from different trophic levels. These studies have shown increases in both farm productivity and the growth rates of co-cultured species, and a reduction in waste products (e.g. Li et al., 1983; Wang, 2001; Chopin et al., 2008; Hughes and Kelly, 2011).

The only commercial scale IMTA operation based on sound scientific research is in the Bay of Fundy in Canada producing salmon and mussels (Chopin et al., 2004; Barrington et al., 2009; Reid et al., 2009). This research commenced in 2001 and at present pilot studies are underway incorporating other species such as sea cucumbers, oysters and sea urchins. Although much of Chilean integrated aquaculture is land-based, the co-culture of blue mussels around open water salmon pens has become common (Soto and Jara, 2007) and trialling of macroalgae culture is also taking place (Buschmann et al., 2008). Being driven by industry rather than scientific research, the placement of the mussel ropes is driven by availability of space as opposed to optimal design (Hughes and Kelly, 2011).

In Scotland there have been a number of experimental/pilot scale trials which have yielded encouraging scientific results, but as yet there is no major commercialisation. Research to date in Scotland has shown that well-designed integrated systems can lead to

* Corresponding author. Tel.: +64 3 3488987; fax: +64 3 3485548.
*E-mail addresses:* j.ren@niwa.co.nz, jeffrey.ren2012@gmail.com (J.S. Ren).

0304-3800/$ – see front matter © 2012 Elsevier B.V. All rights reserved.
http://dx.doi.org/10.1016/j.ecolmodel.2012.07.020

a reduction in nitrogen emissions from caged fish through harvest of sea urchins and seaweeds but for cultured bivalves, the link to fish culture may only be evident where ambient phytoplankton or seston is limiting (Hughes and Kelly, 2011). This highlights the need to consider the influence natural physical and biological variability of the supporting ecosystem in the design of integrated systems of fish, filter-feeding or grazing invertebrates and seaweed.

Biogeochemical fluxes in surrounding water and sediments play an important role in nutrient cycling and affect internal food supply in farming ecosystems which have been explicitly described in many modelling studies on shellfish aquaculture (e.g. Bacher et al., 1998; Grant et al., 2007; Grangeré et al., 2010). As an IMTA operation is much more complex than monoculture, the biomass and production of each trophic species are difficult to optimise economically through the traditional technique of trial and error and experimentation. This present study offers a model framework that considers the influence of natural biogeochemical fluxes over time on the integrated nutritional pathways between IMTA groups and is designed to predict the optimal stocking biomass at each trophic level to produce an effective economic yield. The model incorporates hydrodynamic processes and metabolic energetics of cultured species with an ecological model to design proximal-balanced ecological IMTA units.

Most ecosystem models strive to relate the distribution and fluctuation in abundance and production of wild living organisms to variations in food conditions, predation and the abiotic environment (Fransz et al., 1991). Similarly the IMTA model aims to map out interactions between co-cultured species and their ecosystem components and predict productive capacity. The impact of cultured species on the environment in coastal systems can also be quantitatively and objectively integrated into the model. A few ecosystem models have been developed to assess environmental impact and carrying capacity of farming systems, but most of the model development has focused on monoculture of bivalves (e.g. Bacher et al., 1998; Dowd, 2005; Grant et al., 2007). Some multi-species modelling work has been attempted to study the carrying capacity of a shellfish polyculture system (Duarte et al., 2003). The functioning of polyculture differs from an IMTA system because species from the same trophic level are included in polyculture (e.g. oysters and scallops used in these studies share the same biological and chemical processes which could potentially impact natural phytoplankton populations). Culturing species at the same trophic level does not mitigate environmental impacts (Chopin et al., 2008). IMTA practices strive to facilitate nutrient recycling and optimise co-culture productivity through bioremediation. To achieve this, biomass stocking densities of the culture species must be optimised by means of ecosystem models.

The main focus of this model is to provide a research tool to fine-tune the design of field trials to optimise yields from each trophic level. Model development followed a number of steps. Firstly, we developed an IMTA model based on dynamic energy budgets (DEB) for each trophic grouping within a finfish–shellfish-detritivore-primary producer profile. Secondly, to test the concept and capability of the model, it was parameterised using potential IMTA species namely, salmon, mussels, sea cucumbers and seaweed. Lastly, IMTA scenario simulations were undertaken to understand the dynamics and potential ecological benefits of IMTA farming.

## 2. Model description

The IMTA model incorporates an ecosystem model (Ren et al., 2010) with DEB sub-models for each trophic group within the benthic and pelagic components that interact through carbon and nitrogen budgets and nutrient cycling (Fig. 1). The dynamics of all biological groups, cultured and non-cultured organisms, are described at the population level. For cultured animals, the population energetics depends on that of individuals. Population dynamics of trophic groups are determined by culture strategies and natural mortality. Individuals are removed when reaching a harvest size. Stochastic events may cause additional mortality but are not included in the model.

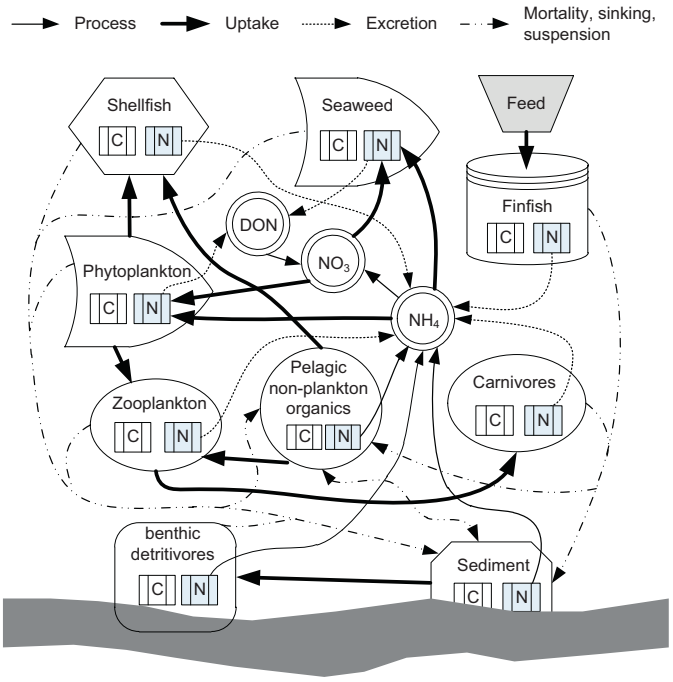


**Fig. 1.** Conceptual diagram of the IMTA model illustrating the coupling of eco-physiological and biogeochemical processes through carbon (C) and nitrogen (N) pathway between the various compartments. The state variables are defined in Table 1 and rate processes listed in Table 2. The cultured trophic group comprises fed organisms (finfish), suspended filtering feeders (shellfish), nutrient extractive organisms (seaweed) and benthic detritivores (sea cucumber). The pelagic compartment includes phytoplankton, zooplankton, carnivore, dissolved inorganic nitrogen (DIN), dissolved organic nitrogen (DON), pelagic non-plankton organic carbon and pelagic non-plankton organic nitrogen. DIN consists of ammonia nitrogen ($NH_4$) and nitrate nitrogen ($NO_3$). The benthic compartment is comprised of carbon sediment and nitrogen sediment.

Nutrients, pelagic organic matter, phytoplankton, zooplankton and carnivores are exchanged between the farming system and adjacent open waters. This was driven by local hydrodynamic processes where exchange rates were dependent on advection by water currents and turbulent diffusion. These were calculated using a separate hydrodynamic model (see Section 3.4). The IMTA model uses a box model concept with divisions in geographic position. Pelagic variables in the pelagic compartment are assumed to be homogeneous within each box. The biomass exchange of the variables between adjacent boxes is determined by exchange coefficients (day$^{-1}$), as $dEx_{ij}/dt = k_{ij}(Ex_i - Ex_j)$ with $k_{ij}$ representing the water volume exchanged from boxes $Ex_i$ to $Ex_j$. The exchange coefficients were based on the results of the 2D hydrodynamic model. A farm ecosystem can be divided into several boxes depending on requirements and local hydrodynamic conditions. The differential equations describing the conservation of state variables are listed in Table 1. The biological intermediate processes are summarised in Table 2 and briefly described below.

### 2.1. Temperature

The rate processes of biological groups are temperature dependent. A single equation ($T_{emp}$) is used to describe the temperature

**Table 1**
System of differential equations.

**Cultured organisms**

Reserves ($j$)

$\frac{dE_*}{dt} = p_{A*} - p_{C*}$

Reproductive reserves ($j$)

$\frac{dE_{R*}}{dt} = (1-\kappa_*)p_{C*} - p_{J*}$

Biovolume growth ($cm^3$)

$\frac{dV_*}{dt} = \frac{(\kappa_* \cdot p_{C*} - p_{M*})_+}{[E_{G*}]}$

Population dynamics (No.)

$\frac{d*N}{dt} = -\delta_{r*} \cdot *N - \delta_{h*} \cdot *N$

Seaweed carbon ($mgC\,m^{-3}$)

$\frac{dCA}{dt} = U_{ca} - r_a T_{empA} CA - (\delta_{ra} + \delta_{ha})CA$

Seaweed nitrogen ($mgN\,m^{-3}$)

$\frac{dNA}{dt} = (1-e_{ua})U_{na} - r_a T_{empA} NA - (\delta_{ra} + \delta_{ha})NA$

**Pelagic organisms**

Carnivore structure weight ($mgC\,m^{-3}$)

$\frac{dCC}{dt} = G_c - CC_\rho \pm Ex_{CC}$

Carnivore reserves (mgC)

$\frac{dEC}{dt} = (1-d_c)U_c - G_c - EC_\rho \pm Ex_{EC}$

Zooplankton structure weight ($mgC\,m^{-3}$)

$\frac{dCZ}{dt} = G_z - CZ_\rho - U_c CZ/(CZ+EZ) \pm Ex_{CZ}$

Zooplankton reserves ($mgC\,m^{-3}$)

$\frac{dEZ}{dt} = (1-d_z)(U_{zp} + U_{zo}) - G_z - EZ_\rho - U_c EZ/(CZ+EZ) \pm Ex_{EZ}$

Phytoplankton carbon ($mgC\,m^{-3}$)

$\frac{dCP}{dt} = U_{cp} - r_p T_{empP} CP - U_{zp} - U_{mp} MN/V - M_p \pm Ex_{CP}$

Phytoplankton nitrogen ($mgN\,m^{-3}$)

$\frac{dNP}{dt} = (1-e_{up})U_{np} - r_p T_{empP} NP - Q_p U_{zp} + Q_p U_{mp} MN/V - Q_p M_p \pm Ex_{NP}$

**Pelagic carbon and nitrogen**

Pelagic non-plankton organic carbon ($mgC\,m^{-3}$)

$\frac{dPOC}{dt} = (1-k_{sr}-k_{db})[Z_f + C_f + F_m MN/V + U_{mo} MN/V + F_f FN/V + F_w FN/V + \gamma_o CS/H - \lambda_o POC] \pm Ex_{POC}$

Pelagic non-plankton organic nitrogen ($mgN\,m^{-3}$)

$\frac{dPON}{dt} = (1-k_{sr}-k_{db})[Q_z Z_f + Q_c C_f + Q_p F_m MN/V + Q_o U_{mo} MN/V + Q_f F_f FN/V + Q_{ff} F_w FN/V + \gamma_o NS/H - \lambda_o PON] \pm Ex_{PON}$

Dissolved organic nitrogen ($mgN\,m^{-3}$)

$\frac{dND}{dt} = \varphi(P_{excr} + A_{excr}) - k_{or} ND \pm Ex_{ND}$

Ammonium nitrogen ($mgN\,m^{-3}$)

$\frac{dNH}{dt} = (1-\varphi)\cdot(P_{excr} + A_{excr}) - U_{np}U_{nhp}/(U_{nop}+U_{nhp}) - U_{na}U_{nha}/(U_{noa}+U_{nha}) - k_{nit} NH + k_{or} ND + k_{sr} NS/H + k_{sr} PON + (MN \cdot M_{excr} + FN \cdot F_{excr} + DN \cdot D_{excr})/V + C_{excr} + Z_{excr} \pm Ex_{NH}$

Nitrate nitrogen ($mgN\,m^{-3}$)

$\frac{dNO}{dt} = k_{nit} NH - U_{np}U_{nop}/(U_{nop}+U_{nhp}) - U_{na}U_{noa}/(U_{noa}+U_{nha}) - k_{denit} NO \pm Ex_{NO}$

**Benthic carbon and nitrogen**

Sediment organic carbon ($mgC\,m^{-2}$)

$\frac{dCS}{dt} = (\lambda_o POC + M_p + M_z + M_c)H + [M_m + M_f + M_d + F_d DN + \delta_{ra} CA]/A - \gamma_o CS - (k_{sr} + k_{db})CS$

Sediment organic nitrogen ($mgN\,m^{-2}$)

$\frac{dNS}{dt} = (\lambda_o PON + Q_p M_p + Q_z M_z + Q_c M_c)H + [Q_m M_m + Q_f M_f + Q_d M_d + Q_s F_d DN + \delta_{ra} NA]/A - \gamma_o NS - (k_{sr} + k_{db})NS$

*Notes*: The expression $(x)_+$ is defined as: $[x]_+ = x$ for $x > 0$, $[x]_+ = 0$ otherwise. * Represents cultured animals: $m$ for shellfish, $f$ for finfish and $d$ for detritovore.

effect on physiological rates of organisms. Within a species-specific optimal range of temperatures, the rate of physiological processes is described by an Arrhenius relationship (Kooijman, 2000) whereby rates increase exponentially with temperature up to an asymptote and then decreases with further increase in temperature. Outside the optimal temperature range, catabolic rates would be considerably reduced and therefore the Arrhenius relationship is extended to cover the temperature-dependent rate processes beyond the lower and upper boundaries. The existing ecosystem model describes the rate processes of pelagic organisms using an exponential function (Ren et al., 2010). Experimental data have indicated that the Arrhenius relationship can better reflect eco-physiological behaviours of organisms (e.g. Goldman, 1977; Fralick et al., 1990; Yurista, 1999; van der Veer et al., 2006). This Arrhenius equation is therefore applied to all biological groups.

### 2.2. Cultured animals

DEB sub-models describe the energetics of cultured animals within the three trophic groupings: fed organisms (finfish), suspended filtering feeders (shellfish) and benthic detritivores (sea cucumber). These sub-models are based on common mechanistic rules that describe the uptake and use of energy. Following DEB theory (Kooijman, 2000), we developed a general framework of DEB model for application to all trophic groups with the difference in species-specific parameter values. The description of a standard DEB model can be found elsewhere (e.g. van der Meer, 2006; Pouvreau et al., 2006) and we only briefly summarise the main outline here.

The energetic of an organism is described by three state variables: biovolume, reserves and reproductive reserves. The difference between biovolume and reserves is that the former only increases when energy allocated for maintenance and growth exceeds maintenance requirements. The latter, however, is replenished from feeding and continuously depleted through catabolism. The rate of energy uptake follows a type-II functional response to food density and is proportional to surface area, whereas maintenance depends on biovolume. The energy acquired from feeding is immediately incorporated into reserves from which it is utilised at a fixed fraction of $\kappa$ for maintenance and growth, while the remaining fraction of $1-\kappa$ is spent on development in juveniles and reproduction in adults. Metabolic maintenance competes for energy with growth but has priority, while development and reproduction compete with growth plus maintenance at a higher level. If the energy allocation with respect to maintenance and growth is less than maintenance cost, growth stops and maintenance need is met by reducing reproduction. The individual would die when the energy utilisation rate from reserves is insufficient to meet the maintenance cost.

The energy allocated to reproduction is stored in a reproductive buffer, converted to eggs at the time of reproduction, emptied at spawning and replenished thereafter. The physiological processes accompanying energy loss as overheads include feeding and digestion, somatic and maturity maintenance, reproduction and biovolume growth. The overheads accompany ammonia excretion.

### 2.3. Seaweed and phytoplankton

Phytoplankton biomass is modelled as primary production with grazing pressure by shellfish and zooplankton, while the biomass of seaweed is modelled as the difference between growth and loss through respiration. The rate processes of both seaweed and phytoplankton are described with similar functional responses. The difference is that phytoplankton biomass in an ecosystem is calculated as a function of physiological processes and exchanges with the sea, while seaweed biomass only depends on physiological processes. N-quota (N:C ratio) of both seaweed and phytoplankton can vary considerably with their environment. Because the uptake of carbon and nitrogen is N-quota dependent, the growth of phytoplankton and seaweed is described by two state variables: carbon and nitrogen. The uptake of carbon is governed by irradiance, temperature and N-quota. Phosphorous and silicon are not considered in the model because they are not usually limiting factors (e.g. Gibbs and Vant, 1997). The model only describes the conservation of carbon and nitrogen.

The uptake of dissolved inorganic nitrogen (DIN) follows a Michaelis–Menten function (Caperon and Meyer, 1972) and is limited by N-quota. A decrease function of maximum uptake rate to N-quota is introduced to prevent the occurrence of an unrealistically high N:C ratio. Seaweed and phytoplankton may release a considerable fraction of production as dissolved organic nitrogen (DON), which is described to be proportional to nutrient uptake and respiration rates. Phytoplankton loss through sinking depends on the N-quota and is proportional to the biomass. Natural mortality and harvest will result in the loss of seaweed biomass.

**Table 2**
Biological intermediate processes.

| Symbol | Description | Formula | Unit |
|---|---|---|---|
| $f_*$ | Functional response of cultured animals * | $X_*/(X_* + X_{H^*})$ | Dimensionless |
| $T_{emp^*}$ | Temperature-dependent rate of biological group* | $k_{0^*}\cdot\exp(T_{A^*}/T_{0^*} - T_{A^*}/T)\cdot[1+\exp(T_{AL^*}/T - T_{AL^*}/T_{L^*}) + \exp(T_{AH^*}/T_{H^*} - T_{AH^*}/T)]^{-1}$ | Dimensionless |
| $U_f$ | Consumption rate of finfish | $T_{empF}\cdot\min(F_r, U_{mf})\cdot V_f^{2/3}$ | mgC d$^{-1}$ |
| $U_{mp}$ | Consumption rate of phytoplankton by shellfish | $T_{empM}\cdot U_{mm}\cdot CP\cdot V_m{}^{2/3}$ | mgC d$^{-1}$ |
| $U_{mo}$ | Consumption rate of POC by shellfish | $T_{empM}\cdot U_{mm}\cdot POC\cdot V_m{}^{2/3}$ | mgC d$^{-1}$ |
| $U_d$ | Consumption rate of sea cucumber | $T_{empD}\cdot f_d\cdot U_{md}\cdot V_d{}^{2/3}$ | mgC d$^{-1}$ |
| $p_{A^*}$ | Assimilation rate of cultured animals * | $T_{emp^*}\cdot f_{*}\cdot\{p_{A^*}\}\cdot V_*{}^{2/3}$ | J d$^{-1}$ |
| $p_{C^*}$ | Catabolic rate of cultured animals * | $T_{emp^*}\cdot[E_*]/([E_{C^*}] + \kappa_{*}\cdot[E_*])]\cdot([E_{G^*}]\cdot\{p_{A^*}\}\cdot V_*{}^{2/3}/[E_{m^*}] + [p_{M^*}]\cdot V_*)$ | J d$^{-1}$ |
| $p_{M^*}$ | Maintenance rate of cultured animals * | $T_{emp^*}\cdot[p_{M^*}]\cdot V_*$ | J d$^{-1}$ |
| $p_{J^*}$ | Maturity maintenance of cultured animals * | $\min(V_*, V_{p^*})\cdot[p_{M^*}]\cdot(1-\kappa_*)/\kappa_*$ | J d$^{-1}$ |
| $F_*$ | Faeces of cultured animals | $U_* - p_{A^*}/\mu_{CJ}$ | mgC d$^{-1}$ |
| $F_w$ | Waste feed | $T_{empF}\cdot(F_r - U_{mf})_+\cdot V_f^{2/3}$ | mgC d$^{-1}$ |
| $F_{excr}$ | Fish excretion | $\{[p_{Cf} - (1-\kappa_{Rf})\cdot dE_{Rf}/dt - \mu_{Vf}\cdot\rho\cdot dV_f/dt]\cdot Q_f + p_{Af}\cdot(\underline{Q_{ff}} - Q_f)_+\}/\mu_{CJ}$ | mgN d$^{-1}$ |
| $M_{excr}$ | Shellfish excretion | $\{[p_{Cm} - (1-\kappa_{Rm})\cdot dE_{Rm}/dt - \mu_{Vm}\cdot\rho\cdot dV_m/dt]\cdot Q_m + p_{Am}\cdot(Q_p - Q_m)_+\}/\mu_{CJ}$ | mgN d$^{-1}$ |
| $D_{excr}$ | Sea cucumber excretion | $\{[p_{Cd} - (1-\kappa_{Rd})\cdot dE_{Rd}/dt - \mu_{Vd}\ \rho dV_d/dt]\cdot Q_d + p_{Ad}\cdot(Q_s - Q_d)_+\}/\mu_{CJ}$ | mgN d$^{-1}$ |
| $M_*$ | C loss (mortality) of biological group * | $\delta_{r^*}{}^*N\cdot[V_{*}\cdot\rho\mu_{V^*} + (E_* + E_{R^*}\cdot\kappa_{R^*})]/\mu_{CJ}$ | mgC d$^{-1}$ |
| $W_*$ | Individual wet weight of cultured animals * | $V_{*}\cdot\rho + (E_* + E_{R^*}\cdot\kappa_{R^*})/\mu_{E^*}$ | g |
| $U_{nha}$ | Potential uptake of ammonium N by seaweed | $U_{nhma}\cdot(NH/(NH + X_{anh}))$ | d$^{-1}$ |
| $U_{noa}$ | Potential uptake of nitrate N by seaweed | $U_{noma}\cdot(NO/(NO + X_{ano}))$ | d$^{-1}$ |
| $L$ | Daily irradiance | $L(t)\cdot\exp\{-[k_{back} + k_p\cdot(CP + CA)]\cdot H\}$ | μmol phot m$^{-2}$ d$^{-1}$ |
| $f\ (L)$ | Irradiance effect on C uptake | $\frac{1}{H}\cdot\int_0^H L/(L + X_l)dz$ | Dimensionless |
| $U_{na}$ | Total uptake of N by seaweed | $NA\cdot T_{empA}\cdot(U_{nha} + U_{noa})/\{1+\exp[(Q_a - Q_{amax})/Q_{aoff}]\}$ | mgN d$^{-1}$ |
| $U_{ca}$ | Uptake of C by seaweed | $f(L)\cdot CA\cdot T_{empA}\cdot G_{am}\cdot(1 - Q_{amin}/Q_a)_+$ | mgC d$^{-1}$ |
| $A_{excr}$ | Seaweed excretion | $e_{ua}\cdot U_{na} + r_a\cdot T_{empA}\cdot CA\cdot Q_a$ | mgN d$^{-1}$ |
| $Q_a$ | Seaweed N quota | $NA/CA$ | mgN mgC$^{-1}$ |
| $W_a$ | Seaweed biomass | $CA/(\mu_{CA}\cdot 10^6)$ | kg m$^{-3}$ |
| $U_c$ | Uptake of C by carnivore | $CC\cdot U_{ccm}\cdot[(CZ + EZ)/(CZ + EZ + X_{Hz})]\cdot\min(Q_z/Q_c, 1)$ | mgC d$^{-1}$ |
| $C_f$ | Carnivore faeces | $d_c\cdot U_c$ | mgC d$^{-1}$ |
| $G_c$ | Carnivore growth rate | $G_{cm}\cdot EC\cdot T_{empC}\cdot\max\{0, 1 - R_{cmin}/[EC/(CC + EC)]\}$ | mgC d$^{-1}$ |
| $EC_\rho$ | C loss rate of carnivore reserves | $\delta_c\cdot EC + r_c\cdot T_{empC}\cdot CC$ | mgN d$^{-1}$ |
| $CC_\rho$ | C loss rate of carnivore structure weight | $\delta_c\cdot CC$ | mgN d$^{-1}$ |
| $C_{excr}$ | Carnivore excretion | $e_{uc}\cdot U_c\cdot Q_c + r_c\cdot T_{empC}\cdot CC\cdot Q_c$ | mgN d$^{-1}$ |
| $M_c$ | Carnivore mortality | $\delta_c\cdot(CC + EC)$ | mgC d$^{-1}$ |
| $W_c$ | Carnivore biomass | $CC + EC$ | mgC m$^{-3}$ |
| $U_{zp}$ | Uptake of phytoplankton C by zooplankton | $CZ\cdot U_{czm}\cdot[CP/(CP + X_{pz})]\cdot\min(Q_p/Q_z, 1)$ | mgC d$^{-1}$ |
| $U_{zo}$ | Uptake of POC by zooplankton | $[CZ\cdot U_{poczm}\cdot POC/(POC + X_{pocz})]\cdot min(Q_o/Q_z, 1)$ | mgC d$^{-1}$ |
| $G_z$ | Zooplankton growth rate | $G_{zm}\cdot EZ\cdot T_{empZ}\cdot\max\{0, 1 - R_{zmin}/[EZ/(CZ + EZ)]\}$ | mgC d$^{-1}$ |
| $Z_f$ | Zooplankton faeces | $d_z\cdot U_{zp} + d_z\cdot U_{zo}$ | mgC d$^{-1}$ |
| $EZ_\rho$ | C loss rate of zooplankton reserves | $\delta_z\cdot EZ + r_z\cdot T_{empZ}\cdot CZ$ | mgN d$^{-1}$ |
| $CZ_\rho$ | C loss rate of zooplankton structure weight | $\delta_z\cdot CZ$ | mgN d$^{-1}$ |
| $Z_{excr}$ | Zooplankton excretion | $e_{uz}\cdot U_z\cdot Q_z + r_z\cdot T_{empZ}\cdot CZ\cdot Q_z$ | mgN d$^{-1}$ |
| $M_z$ | Zooplankton mortality | $\delta_z\cdot(CZ + EZ)$ | mgC d$^{-1}$ |
| $W_z$ | Zooplankton biomass | $CZ + EZ$ | mgC m$^{-3}$ |
| $U_{nhp}$ | Potential uptake of $NH_4$ by phytoplankton | $U_{nhmp}\cdot(NH/(NH + X_{pnh}))$ | d$^{-1}$ |
| $U_{nop}$ | Potential uptake of $NO_3$ by phytoplankton | $U_{nomp}\cdot(NO/(NO + X_{pno}))$ | d$^{-1}$ |
| $U_{np}$ | Total uptake of N by phytoplankton | $NP\cdot T_{empP}\cdot(U_{nhp} + U_{nop})/\{1+\exp[(Q_p - Q_{pmax})/Q_{poff}]\}$ | mgN d$^{-1}$ |
| $U_{cp}$ | Uptake of C by phytoplankton | $f(L)\cdot CP\cdot T_{empP}\cdot G_{pm}\cdot(1 - Q_{pmin}/Q_p)_+$ | mgC d$^{-1}$ |
| $P_{excr}$ | Phytoplankton excretion | $e_{up}\cdot U_{np} + r_p\cdot T_{empP}\cdot CP\cdot Q_p$ | mgN d$^{-1}$ |
| $Q_p$ | Phytoplankton N quota | $NP/CP$ | mgN mgC$^{-1}$ |
| $M_p$ | Phytoplankton C sinking rate | $CP\cdot[\delta_{pmin} + \delta_p\cdot(Q_{pmax} - Q_p)_+]$ | mgC d$^{-1}$ |
| $Q_s$ | Sediment N quota | $NS/CS$ | mgN mgC$^{-1}$ |

*Notes*: The expression $(x)_+$ is defined as: $[x]_+ = x$ for $x > 0$, $[x]_+ = 0$ otherwise. * Represents biological groups: a for seaweed, *p* for phytoplankton, *m* for shellfish, *f* for fish, *d* for sea cucumber, *z* for zooplankton and *c* for carnivore.

Light intensity decreases exponentially with depth with the light extinction coefficient varying with turbidity and shading from the phytoplankton and seaweed. For simplicity, light intensity was described as an exponential function of depth and the biomass of phytoplankton and seaweed.

### 2.4. Zooplankton and carnivores

The dynamic of zooplankton and carnivores has been described by Ren et al. (2010) and is only briefly presented here. We have made a few improvements to the equations describing the energy loss for respiration and effect of temperature on rate processes. The energy required by respiration comes from the reserves and is proportional to structural biomass. Two state variables are used to describe the population dynamic: reserves and structure weight. The rate of energy uptake follows Type-II functional response to food density and is proportional to structure weight. The assimilated energy directly contributes to the reserves which are then used for respiration and structure growth. Zooplankton compete with shellfish for phytoplankton and other pelagic organic matters. Carnivores are assumed to prey exclusively on zooplankton and the energetic is modelled the same as for zooplankton. The ingested carbon is assimilated with a fixed efficiency. Respiration and food uptake accompany N-excretion, which contributes to DIN.

### 2.5. Pelagic non-plankton organic matter

For the present model, the dynamic of pelagic non-plankton organic matter (POM) is explicitly described with two state variables: pelagic non-plankton organic carbon (POC) and pelagic non-plankton organic nitrogen (PON). A major source contributing to POM is faeces produced by zooplankton, carnivores, shellfish and

finfish. Added to this source are waste feed from finfish culture and the pseudofaeces produced by shellfish. Other suspended organic particles exchanged from boundaries also affect the dynamic of POM. Resuspension of sediment organic matter from the benthic compartment represents an organic flux into the water column driven by current velocity and bottom drag of local hydrodynamics. To avoid a detailed sediment model, the resuspension rate is assumed to be the first order of sediment organic matter. Because many aquaculture farms are located at a water depth >20 m in New Zealand, this assumption is unlikely to compromise the calculated organic flux from sediment to pelagic compartments. The unit in the pelagic form is represented as the concentration on a per volume basis, while that in the sediment form is measured as mass per unit area. Thus the mass flux between the pelagic and sediment compartments is adjusted with the water depth (H).

### 2.6. Dissolved nutrients

Nitrate and ammonia are two forms of DIN which are explicitly described in the model. Both phytoplankton and seaweed take up nitrogen from the DIN compartment and release DON. Excretion from both cultured and non-cultured animals is returned directly to the DIN compartment and is readily available for phytoplankton and seaweed growth. POM undergoes breakdown processes and contributes to the nutrient pool in pelagic compartment, which is described as first order process of POM concentration. Similarly, remineralisation of sediment organic matter in the benthic compartment would also result in the release of nutrients into the water column. The N is fully conserved as it flows within the system apart from prescribed loss processes. For the detailed description of nutrient cycling, please see Ren et al. (2010).

### 2.7. Benthic sediment

Net flux of sediment carbon and nitrogen is usually governed by rates of sedimentation and remineralisation of organic sources. There are a few sources contributing to the sediment including faeces, pseudofaeces, waste feed, phytoplankton sinking, dead animals and seaweeds. The settling rate depends on the size and characteristics of the particles. Because corpses of biological groups sink with high rates (e.g. Piedecausa et al., 2009), they are assumed to directly settle onto the seabed. The sinking of the rest organic matters is assumed to be proportional to their pelagic biomass. Since the pelagic component is volume-based while the benthic is area-based, the depth factor is introduced into calculations of mass flux between the two. The biophysical processes of remineralisation and resuspension impose dynamic fluctuations on the amount of carbon and nitrogen in the benthic compartment. Introducing benthic detritivores such as sea cucumbers, which process large quantities of sediment to extract organic matter, adds to the dynamic of these processes and influences the carbon and nitrogen contents.

### 2.8. IMTA mass balance

The principle of an IMTA practice is twofold: to recycle farm-derived wastes from principal species into harvestable production and to reduce environmental impacts. The main waste products are inorganic nutrients and organic particles of waste feed and faeces from finfish, and faeces and pseudofaeces from shellfish (see Table 2). Ideally, the rate of nutrient uptake by the primary producer (seaweed) should equal the excretion rate of the principal aquaculture species. Similarly, the biodeposition rate should not exceed the consumption rate of benthic detritivores. There is some loss of organic waste through biogeochemical processes in both pelagic and benthic form, but the loss from organic to inorganic forms is a small proportion (~1%). For simplicity, this portion is not considered in calculating the mass balance. In this ideal situation, the mass in the system is balanced by:

$$\frac{dU_{nha}}{dt} - \frac{d(F_{excr} + M_{excr})}{dt} = 0 \quad (1)$$

$$\frac{dU_d}{dt} - \frac{d(F_w + F_f + F_m)}{dt} = 0 \quad (2)$$

where $U_{nha}$, $F_{excr}$ and $M_{excr}$ are respectively, ammonia uptake by seaweeds, finfish excretion and shellfish excretion. $U_d$, $F_w$, $F_f$ and $F_m$ are respectively, carbon uptake by benthic detritivores, waste feed, fish faeces, and shellfish faeces plus pseudofaeces.

The nutrient reduction efficiency is simply calculated by:

$$E_{NH} = \frac{dU_{nha}/dt}{d(F_{excr} + M_{excr})/dt} \cdot 100\% \quad (3)$$

Similarly, the waste organic reduction efficiency is estimated by

$$E_O = \frac{dU_d/dt}{d(F_w + F_f + F_m)/dt} \cdot 100\% \quad (4)$$

## 3. Application

### 3.1. Parameterisation

To understand the dynamics of the model and to conduct scenario simulations, we parameterised the model with salmon, mussels, sea cucumber and seaweed. Parameter values and sources are listed in Table 3. Values of most parameters in the pelagic submodels are discussed by Ren et al. (2010). Because the temperature effect on rate processes was modified from the exponential function to the Arrhenius equation, this structural modification requires a new estimation of related parameter values.

Existing information on physiology of the salmon species farmed in New Zealand, *Oncorhynchus tshawytscha* (chinook salmon) is insufficient for estimating the parameters for the finfish trophic box and therefore published physiological data on Atlantic salmon (*Salmo salar*) were used to parameterise feeding and energy acquisition (Stead et al., 1999; Finstad et al., 2004). The energy content of salmon wet weight has been recorded in a range of 4.4–6.4 J $mg^{-1}$ (Finstad et al., 2004) and a fish generally comprises 40% structural weight and 60% of reserves (Kleiber, 1961). This information was used to estimate the parameters related to growth and reserve density. Lack of comprehensive temperature data necessitated a slight modification of the temperature function where the species-specific tolerance range for low and high temperatures was excluded. The catabolic flux coefficient ($\kappa$) for growth and maintenance was estimated indirectly from gonad somatic index information, following van der Meer (2006). The half-saturation coefficient ($X_{Hf}$) for food concentration describing the functional response of energy acquisition rate could not be readily obtained, because it varies with energy content of fish feed. This parameter is treated as a calibration parameter and is discussed in the next section.

For the detritivore trophic box a DEB model which quantitatively describes feeding, growth and energetic was developed for the Asian sea cucumber *Stichopus japonicus* (Ren et al., in prep). Once the physiological energetics for the New Zealand indigenous sea cucumber *Australostichops mollis* are known, they can be substituted into the detritivore box. Similarly, as data for estimating parameters for the indigenous seaweed *Eklonia radiata* are insufficient, values were derived from other seaweed species (see Table 3). For mussels the locally farmed species *Perna canaliculus* has been intensively studied (Ren and Ross, 2005; Ren et al., 2010) and most parameter values are directly taken from these studies.

**Table 3**
Parameters of the IMTA model.

| Parameters | Description | Value | Dimension | Source |
|---|---|---|---|---|
| $T_{Af}$ | Arrhenius temperature of salmon | 6400 | K | Munch and Conover (2002) |
| $k_{0f}$ | Reference physiological reaction rate for salmon at 288 K | 1 | Dimensionless | This study |
| $[E_{mf}]$ | Maximum reserve density of salmon | 11,600 | J cm$^{-3}$ | Finstad et al. (2004) |
| $[E_{Gf}]$ | Volume-specific costs for salmon growth | 6200 | J cm$^{-3}$ | Finstad et al. (2004) |
| $V_{pf}$ | Salmon structural volume at puberty | 9 | cm$^3$ | Graynoth (1995) |
| $X_{Hf}$ | Half-saturation uptake of food by salmon | 5 | g | Calibrated |
| $U_{mf}$ | Salmon maximum surface area-specific consumption | 380 | mgC cm$^{-2}$ d$^{-1}$ | Beauchamp et al. (2007) |
| $\{p_{Af}\}$ | Salmon maximum surface area-specific assimilation | 2250 | J cm$^{-2}$ d$^{-1}$ | Amundsen et al. (1999) |
| $[p_{Mf}]$ | Volume-specific maintenance rate of salmon | 75.3 | J cm$^{-3}$ d$^{-1}$ | Stevens et al. (1998) |
| $\kappa_f$ | Catabolic flux to growth and maintenance in salmon | 0.85 | Dimensionless | This study |
| $\kappa_{Rf}$ | Reproductive reserves fixed in salmon eggs | 0.8 | Dimensionless | This study |
| $\mu_{Ef}$ | Reserve energy content of salmon | 7730 | J g$^{-1}$ wet W | Finstad et al. (2004) |
| $\mu_{Vf}$ | Structure energy content of salmon | 4400 | J g$^{-1}$ wet W | Finstad et al. (2004) |
| $Q_f$ | N-quota of salmon | 0.18 | mgN mgC$^{-1}$ | Redfield ratio |
| $Q_{ff}$ | N-quota of salmon feed | 0.18 | mgN mgC$^{-1}$ | This study |
| $T_{Am}$ | Arrhenius temperature of mussel | 5530 | K | Hickman (1979) |
| $T_{Lm}$ | Lower boundary of tolerance range for mussel | 285 | K | Marsden and Weatherhead (1999) |
| $T_{Hm}$ | Upper boundary of tolerance range for mussel | 297 | K | Marsden and Weatherhead (1999) |
| $T_{ALm}$ | Arrhenius temperature at lower boundary for mussel | 15,000 | K | Marsden and Weatherhead (1999) |
| $T_{AHm}$ | Arrhenius temperature at upper boundary for mussel | 42,000 | K | Marsden and Weatherhead (1999) |
| $k_{0m}$ | Reference reaction rate for mussel at 288 K | 1 | Dimensionless | Ren et al. (2010) |
| $[E_{mm}]$ | Maximum reserve density of mussel | 2600 | J cm$^{-3}$ | Ren et al. (2010) |
| $[E_{Gm}]$ | Volume-specific costs for mussel growth | 2500 | J cm$^{-3}$ | Ren et al. (2010) |
| $V_{pm}$ | Mussel structure volume at puberty | 0.36 | cm$^3$ | Alfaro (2001) |
| $X_{Hm}$ | Half-saturation uptake of phytoplankton by mussels | 315 | mgC m$^{-3}$ | Calibrated |
| $U_{mm}$ | Mussel maximum surface area-specific clearance | 0.045 | m$^3$ cm$^{-2}$ d$^{-1}$ | Hawkins et al. (1999) |
| $\{p_{Am}\}$ | Mussel maximum surface area-specific assimilation | 440 | J cm$^{-2}$ d$^{-1}$ | Hawkins et al. (1999) |
| $[p_{Mm}]$ | Volume-specific maintenance rate of mussel | 12.2 | J cm$^{-3}$ d$^{-1}$ | Marsden and Weatherhead (1999) |
| $\kappa_m$ | Catabolic flux to growth and maintenance in mussel | 0.7 | Dimensionless | Ren et al. (2010) |
| $\kappa_{Rm}$ | Reproductive reserves fixed in mussel eggs | 0.8 | Dimensionless | Ren and Ross (2005) |
| $\mu_{Em}$ | Reserve energy content of mussel | 4500 | J g$^{-1}$ wet W | Ren unpubl. data |
| $\mu_{Vm}$ | Structure energy content of mussel | 2700 | J g$^{-1}$ wet W | Ren unpubl. data |
| $\mu_{CJ}$ | Ratio of carbon to energy content | 48.8 | J mgC$^{-1}$ | This study |
| $Q_m$ | N-quota of mussels | 0.183 | mgN mgC$^{-1}$ | Smaal and Vonck (1997) |
| $\rho$ | Biovolume density of cultured animals | 1 | g cm$^{-3}$ | This study |
| $T_{Ad}$ | Arrhenius temperature of sea cucumber | 7300 | K | Ren, in prep. |
| $T_{Ld}$ | Lower boundary of tolerance range of sea cucumber | 270 | K | Ren, in prep. |
| $T_{Hd}$ | Upper boundary of tolerance range for sea cucumber | 291 | K | Ren, in prep. |
| $T_{ALd}$ | Arrhenius temperature at lower boundary for sea cucumber | 35,500 | K | Ren, in prep. |
| $T_{AHd}$ | Arrhenius temperature at upper boundary for sea cucumber | 70,000 | K | Ren, in prep. |
| $k_{0d}$ | Reference reaction rate for sea cucumber at 288 K | 1 | Dimensionless | Ren, in prep. |
| $[E_{md}]$ | Maximum reserve density of sea cucumber | 1350 | J cm$^{-3}$ | Ren, in prep. |
| $[E_{Gd}]$ | Volume-specific costs for sea cucumber growth | 1260 | J cm$^{-3}$ | Ren, in prep. |
| $V_{pd}$ | Sea cucumber structural volume at puberty | 4.6 | cm$^3$ | Ren, in prep. |
| $X_{Hd}$ | Half-saturation uptake of food by sea cucumber | 50 | gC m$^{-2}$ | Calibrated |
| $U_{md}$ | Sea cucumber maximum surface area-specific consumption | 660 | mgC cm$^{-2}$ d$^{-1}$ | Ren, in prep. |
| $\{p_{Ad}\}$ | Sea cucumber maximum surface area-specific assimilation | 154 | J cm$^{-2}$ d$^{-1}$ | Ren, in prep. |
| $[p_{Md}]$ | Volume-specific maintenance rate of sea cucumber | 4.79 | J cm$^{-3}$ d$^{-1}$ | Ren, in prep. |
| $\kappa_d$ | Catabolic flux to growth and maintenance in sea cucumber | 0.85 | Dimensionless | Ren, in prep. |
| $\kappa_{Rd}$ | Reproductive reserves fixed in sea cucumber eggs | 0.8 | Dimensionless | Ren, in prep. |
| $\mu_{Ed}$ | Reserve energy content of sea cucumber | 900 | J g$^{-1}$ wet W | Ren, in prep. |
| $\mu_{Vd}$ | Structure energy content of sea cucumber | 900 | J g$^{-1}$ wet W | Ren, in prep. |
| $Q_d$ | N-quota of sea cucumber | 0.18 | mgN mgC$^{-1}$ | Redfield ratio |
| $T_{Aa}$ | Arrhenius temperature of seaweed | 8400 | K | Fralick et al. (1990) |
| $T_{La}$ | Lower boundary of tolerance range for seaweed | 287 | K | Fralick et al. (1990) |
| $T_{Ha}$ | Upper boundary of tolerance range for seaweed | 296 | K | Fralick et al. (1990) |
| $T_{ALa}$ | Arrhenius temperature at lower boundary for seaweed | 5000 | K | Fralick et al. (1990) |
| $T_{AHa}$ | Arrhenius temperature at upper boundary for seaweed | 19,000 | K | Fralick et al. (1990) |
| $k_{0a}$ | Reference reaction rate for seaweed at 286 K | 1 | Dimensionless | This study |
| $U_{nhma}$ | Seaweed maximum uptake of ammonia N | 0.02 | d$^{-1}$ | Taylor and Rees (1999) |
| $U_{noma}$ | Seaweed maximum uptake of nitrate N | 0.02 | d$^{-1}$ | Taylor and Rees (1999) |
| $X_{anh}$ | Half-saturation ammonia-N for seaweed uptake | 28 | mgN m$^{-3}$ | As for phytoplankton |
| $X_{ano}$ | Half-saturation nitrate-N for seaweed uptake | 5 | mgN m$^{-3}$ | As for phytoplankton |
| $Q_{amax}$ | Maximum seaweed N:C ratio | 0.2 | mgN mgC$^{-1}$ | Calibrated |
| $Q_{amin}$ | Minimum seaweed N:C ratio | 0.1 | mgN mgC$^{-1}$ | Calibrated |
| $Q_{aoff}$ | Seaweed nitrogen uptake parameter | 0.03 | mgN mgC$^{-1}$ | Calibrated |
| $G_{am}$ | Maximum seaweed growth rate | 0.04 | d$^{-1}$ | Mao et al. (1993) |
| $r_a$ | Respiration rate of seaweed | $2 \times 10^{-4}$ | d$^{-1}$ | Calibrated |
| $e_{ua}$ | Uptake associated excretion of seaweed | 0.01 | Dimensionless | Calibrated |
| $\varphi$ | DON fraction of phytoplankton/seaweed excretion | 0.1 | Dimensionless | Pujo-Pay et al. (1997) |
| $\mu_{CA}$ | Carbon to dry weight ratio of seaweed | 0.3 | gC g$^{-1}$ | Duarte and Ferreira (1993) |
| $T_{Ap}$ | Arrhenius temperature of phytoplankton | 6800 | K | Goldman (1977) |
| $T_{Lp}$ | Lower boundary of tolerance range for phytoplankton | 286 | K | Goldman (1977) |
| $T_{Hp}$ | Upper boundary of tolerance range for phytoplankton | 298 | K | Goldman (1977) |
| $T_{ALp}$ | Arrhenius temperature at lower boundary for phytoplankton | 27,300 | K | Goldman (1977) |
| $T_{AHp}$ | Arrhenius temperature at upper boundary for phytoplankton | 80,300 | K | Goldman (1977) |

Table 3 (*Continued*)

| Parameters | Description | Value | Dimension | Source |
|---|---|---|---|---|
| $k_{0p}$ | Reference reaction rate for phytoplankton at 292 K | 1 | Dimensionless | This study |
| $k_{back}$ | Background attenuation coefficient | 0.22 | $m^{-1}$ | Tyler (1983) |
| $X_l$ | Half-saturation light level | 7 | $\mu mol\ phot\ m^{-2}\ d^{-1}$ | Kiefer (1990) |
| $k_p$ | Light attenuation coefficient | 0.01 | $mgC^{-1}\ m^2$ | Tyler (1983) |
| $U_{nhmp}$ | Phytoplankton maximum uptake of $NH_4$-N | 0.55 | $d^{-1}$ | Caperon and Meyer (1972) |
| $U_{nomp}$ | Phytoplankton maximum uptake of $NO_3$-N | 0.45 | $d^{-1}$ | Caperon and Meyer (1972) |
| $X_{pnh}$ | Half-saturation $NH_4$-N for phytoplankton uptake | 28 | $mgN\ m^{-3}$ | Andersen and Nival (1987) |
| $X_{pno}$ | Half-saturation $NH_4$-N for phytoplankton uptake | 5 | $mgN\ m^{-3}$ | Caperon and Meyer (1972) |
| $Q_{pmax}$ | Maximum phytoplankton N:C ratio | 0.25 | $mgN\ mgC^{-1}$ | Tett and Droop (1988) |
| $Q_{pmin}$ | Minimum phytoplankton N:C ratio | 0.1 | $mgN\ mgC^{-1}$ | Tett and Droop (1988) |
| $Q_{poff}$ | Phytoplankton nitrogen uptake parameter | 0.01 | $mgN\ mgC^{-1}$ | Ross et al. (1993) |
| $G_{pm}$ | Maximum phytoplankton growth rate | 1.6 | $d^{-1}$ | Caperon and Meyer (1972) |
| $r_p$ | Respiration rate of phytoplankton | 0.01 | $d^{-1}$ | Chapelle et al. (1994) |
| $e_{up}$ | Uptake associated excretion of phytoplankton | 0.05 | Dimensionless | Zlotnik and Dubinsky (1989) |
| $\delta_{pmin}$ | Minimum phytoplankton sinking rate | 0.1 | $d^{-1}$ | Bienfang (1977) |
| $\delta_p$ | Maximum phytoplankton sinking rate | 0.25 | $d^{-1}$ | Tett and Droop (1988) |
| $T_{Ac}$ | Arrhenius temperature of jellyfish | 7100 | K | Widmer (2005) |
| $T_{Lc}$ | Lower boundary of tolerance range for jellyfish | 283 | K | Widmer (2005) |
| $T_{Hc}$ | Upper boundary of tolerance range for jellyfish | 296 | K | Widmer (2005) |
| $T_{ALc}$ | Arrhenius temperature at lower boundary for jellyfish | 3200 | K | Widmer (2005) |
| $T_{AHc}$ | Arrhenius temperature at upper boundary for jellyfish | 32,000 | K | Widmer (2005) |
| $k_{0c}$ | Reference reaction rate for jellyfish at 283 K | 1 | Dimensionless | This study |
| $U_{ccm}$ | Maximum uptake rate of jellyfish | 15 | $d^{-1}$ | Kiørboe et al. (1985) |
| $X_{Hz}$ | Half-saturation uptake of zooplankton by jellyfish | 150 | $mgC\ m^{-3}$ | Kiørboe et al. (1985) |
| $d_c$ | Jellyfish faeces | 0.5 | Dimensionless | Reeve (1980) |
| $R_{cmin}$ | Minimum reserves for jellyfish growth | 0.3 | Dimensionless | Ren et al. (2010) |
| $G_{cm}$ | Maximum growth rate of jellyfish | 0.1 | $d^{-1}$ | Møller and Riisgård (2007) |
| $\delta_c$ | Jellyfish mortality | 0.05 | $d^{-1}$ | Ross et al. (1993) |
| $Q_c$ | N-quota of jellyfish | 0.18 | $mgN\ mgC^{-1}$ | Redfield ratio |
| $r_c$ | Respiration rate of jellyfish | 0.1 | $d^{-1}$ | Møller and Riisgård (2007) |
| $e_{uc}$ | Uptake associated excretion of jellyfish | 0.15 | Dimensionless | Kiørboe et al. (1985) |
| $T_{Az}$ | Arrhenius temperature of zooplankton | 6200 | K | Yurista (1999) |
| $T_{Lz}$ | Lower boundary of tolerance range for zooplankton | 288 | K | Yurista (1999) |
| $T_{Hz}$ | Upper boundary of tolerance range for zooplankton | 302 | K | Yurista (1999) |
| $T_{ALz}$ | Arrhenius temperature at lower boundary for zooplankton | 5100 | K | Yurista (1999) |
| $T_{AHz}$ | Arrhenius temperature at upper boundary for zooplankton | 47,000 | K | Yurista (1999) |
| $k_{0z}$ | Reference reaction rate for zooplankton at 291 K | 1 | Dimensionless | This study |
| $U_{czm}$ | Maximum uptake rate of phytoplankton by zooplankton | 2 | $d^{-1}$ | Kiørboe et al. (1985) |
| $U_{poczm}$ | Maximum uptake rate of POC by zooplankton | 0.5 | $d^{-1}$ | This study |
| $X_{pz}$ | Half-saturation uptake of phytoplankton by zooplankton | 150 | $mgC\ m^{-3}$ | Kiørboe et al. (1985) |
| $X_{pocz}$ | Half-saturation uptake of POC by zooplankton | 300 | $mgC\ m^{-3}$ | This study |
| $d_z$ | Zooplankton faeces | 0.25 | Dimensionless | Kiørboe et al. (1985) |
| $R_{zmin}$ | Minimum reserves for zooplankton growth | 0.3 | Dimensionless | Ren et al. (2010) |
| $G_{zm}$ | Maximum growth rate of zooplankton | 0.1 | $d^{-1}$ | Møller and Riisgård (2007) |
| $\delta_z$ | Zooplankton mortality | 0.05 | $d^{-1}$ | Corkett and Maclaren (1979) |
| $Q_z$ | N-quota of zooplankton | 0.18 | $mgN\ mgC^{-1}$ | Redfield ratio |
| $Q_o$ | N-quota of particulate detrital organics | 0.18 | $mgN\ mgC^{-1}$ | Redfield ratio |
| $r_z$ | Respiration rate of zooplankton | 0.02 | $d^{-1}$ | Nakata et al. (2000) |
| $e_{uz}$ | Uptake associated excretion of zooplankton | 0.15 | Dimensionless | Kiørboe et al. (1985) |
| $k_{nit}$ | Water-column nitrification rate | 0.1 | $d^{-1}$ | Chapelle (1995) |
| $k_{denit}$ | Water-column denitrification rate | 0.02 | $d^{-1}$ | Devola et al. (2006) |
| $k_{db}$ | Sediment N and C bury rate | 0.001 | $d^{-1}$ | Ren et al. (2010) |
| $k_{or}$ | Water-column DON remineralisation rate | 0.022 | $d^{-1}$ | Dutkiewicz et al. (2001) |
| $k_{sr}$ | Nitrogen and carbon release rate | 0.01 | $d^{-1}$ | Edwards and Grantham (1986) |
| $\gamma_o$ | Resuspension coefficient of sediment organic matters | 0.01 | $d^{-1}$ | This study |
| $\lambda_o$ | Water-column organic settling rate | 0.05 | $d^{-1}$ | Dowd (2005) |
| $\delta_{ra}$ | Natural mortality of seaweed | 0.001 | $d^{-1}$ | Dowd (2005) |
| $\delta_{rf}$ | Natural mortality of salmon | 0.001 | $d^{-1}$ | Dowd (2005) |
| $\delta_{rm}$ | Natural mortality of mussels | 0.001 | $d^{-1}$ | Dowd (2005) |
| $\delta_{rd}$ | Natural mortality of sea cucumber | 0.001 | $d^{-1}$ | Ren, in prep. |

### 3.2. Study area and observational data

To provide biophysical data for the IMTA model, water samples were collected from two bays supporting salmon and mussel farming at 6 weekly intervals for one year (March 2007 to April 2008). The bays were Waihinau Bay and Port Ligar, located off the main channel of Pelorus Sound at the northern end of the South Island of New Zealand (Fig. 2). The salmon farm is in western Waihinau Bay where it covers a small area ($\sim 9 \times 10^3\ m^2$) compared to the total bay area of $2.3 \times 10^6\ m^2$. Port Ligar has an extensive amount of mussel farming (by New Zealand standards) with farms occupying $8.8 \times 10^5\ m^2$ compared to the bay area of $8.3 \times 10^6\ m^2$.

Water samples were collected within both fish and mussel farms, along transect lines away from farms and at the main channel of Pelorus Sound using a tube sampler (25 mm diameter, 15 m length). Water samples were analysed for chlorophyll-*a*, particulate organic carbon (POC), particulate organic nitrogen (PON), ammonium nitrogen ($NH_4$), and nitrate nitrogen ($NO_3$). At each sampling site, a CTD profile of temperature and salinity was taken. Current measurements were taken at a number of sites in the bays and around the farms to develop a hydrodynamic model. The growth of

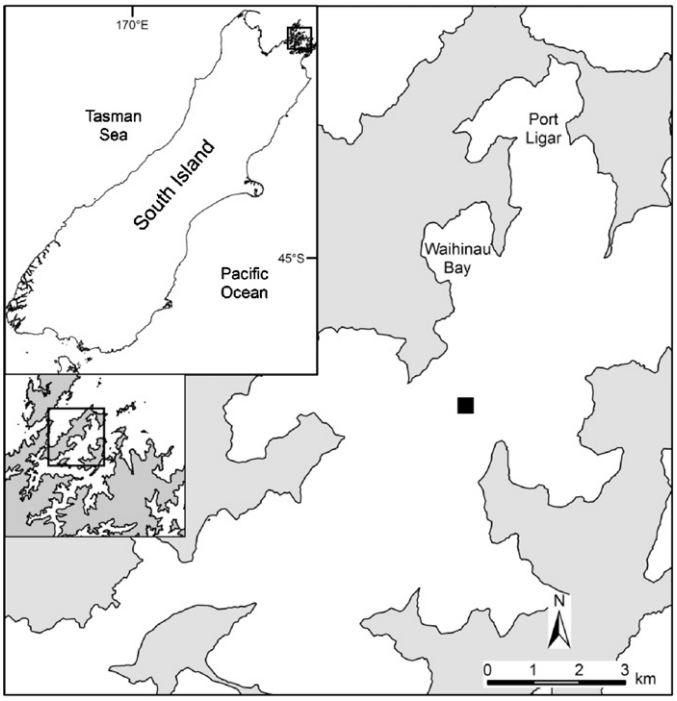


**Fig. 2.** Location of the study area, Waihinau Bay and Port Ligar in Pelorus Sound, New Zealand. The square shows the sampling point in the main channel of Pelorus Sound.

mussels was also conducted at both fish and mussel farms during this period.

### 3.3. Model setup

After parameterisation, each of the DEB sub-models were independently calibrated using growth and environmental data. The most uncertain parameter is the half-saturation coefficients ($X_{H^*}$) which depend on food quality and quantity. Because it is not possible to directly estimate these values, they were treated as calibration parameters, following Pouvreau et al. (2006). These sub-models were then integrated into the modified ecosystem model (Ren et al., 2010) to form the framework of an IMTA model to simulate the yield of the principal species (salmon and mussels) and secondary species (sea cucumbers and seaweed).

The field data were used for a crude validation of the model. The model simulations were based on standard farming practices. The mussel farm was based on ~1.5 backbones per hectare with three mussel cohorts at a farming site at any one time. To be consistent with culture practice, the model simulation was designed to include small, medium and large mussels with lengths of 25, 55 and 75 mm at densities of 180, 150 and 120 per metre longline, respectively. Mussel numbers in each cohort was calculated according to the farm area. For salmon culture, the farming company provided data on stocking density and husbandry information. Because this information is confidential, the stocking density is presented in terms of a biomass index (Fig. 3). The initial values of sediment-N were set to zero for model runs and pelagic variables from the main channel of Pelorus Sound were used for the boundary flux conditions. Because the farming areas are relatively small, we set one box for both the fish and mussel farms.

After calibration, the model is subsequently used to simulate IMTA scenarios to estimate stocking densities of biomitigators (seaweed and sea cucumbers) and investigate ecological benefits for conversion from monoculture to IMTA practices. Scenario simulations were based on existing culture practices by assuming that the

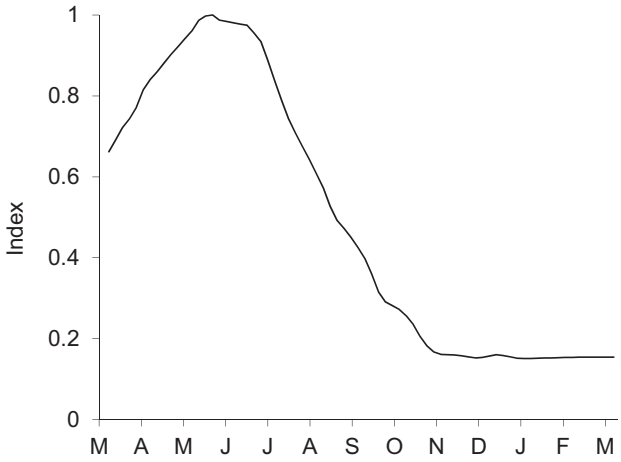


**Fig. 3.** Index of salmon biomass in Waihinau Bay during March 2007 and April 2008.

current monoculture is converted into an IMTA practice through introduction of co-cultured species into the system. The stocking density of mussels remains unchanged in Port Ligar. For the salmon site in Waihinau Bay, however, general culture information from salmon industry was used so that the number of fish in each cohort was set to $1.2 \times 10^5$ individuals. The stock of sea cucumbers was assumed to consist of three cohorts with initial individual weights of 50, 100 and 150 g, respectively. The initial salmon stock also consisted of three cohorts with length of 20, 25 and 30 cm corresponding with body weight of 110 g, 225 g and 400 g. Natural mortality ($\delta_r$) was set at 0.1% for all cultured animals and harvesting mortality was set to 1 at the time of harvesting, but was not considered throughout the simulation period. Ideally, an optimised IMTA system should convert all farm-derived waste into harvestable biomass. Practically, the waste would not be fully utilised by biomitigators during the entire culture period due to the difference in environmental effects on rate processes between animals. For model runs, the initial biomasses of seaweed and sea cucumbers are arbitrarily set and optimised until the farm-derived wastes are reduced to 'equilibrium' low levels. A few criteria are followed to decide the optimal biomass: (1) the values from Eqs. (1) and (2) (in Section 2.8) should always be less than or equal to 0; and (2) the values from Eqs. (3) and (4) are between 0–100% and should be as close to 100% as possible.

### 3.4. Hydrodynamics

The IMTA model is not spatially explicit, but uses a number of benthic and pelagic compartments with exchanges between these boxes. A hydrodynamic model was used to firstly estimate appropriate sizes for the benthic and pelagic compartments, and then to calculate the flows into and between compartments. The hydrodynamic model is described in detail elsewhere (Plew, 2011). In brief, a 2D finite element hydrodynamic model with an unstructured grid and resolution varying between 5 and 10 km offshore and 25 m in the study area was used to simulate the tidally driven currents. To calculate the sizes of the benthic compartments associated with deposition from the fish and mussel farms, a particle tracking and dispersal algorithm was embedded into the hydrodynamic model. Particles were continuously released within farm areas for 72 h and tracked until they reached the seabed. The sinking velocity of 4 cm $s^{-1}$ and 2.5 cm $s^{-1}$ was used, respectively for particles from finfish and mussels. The sizes of the benthic compartments were defined as the area within which 90% of the particles are settled.

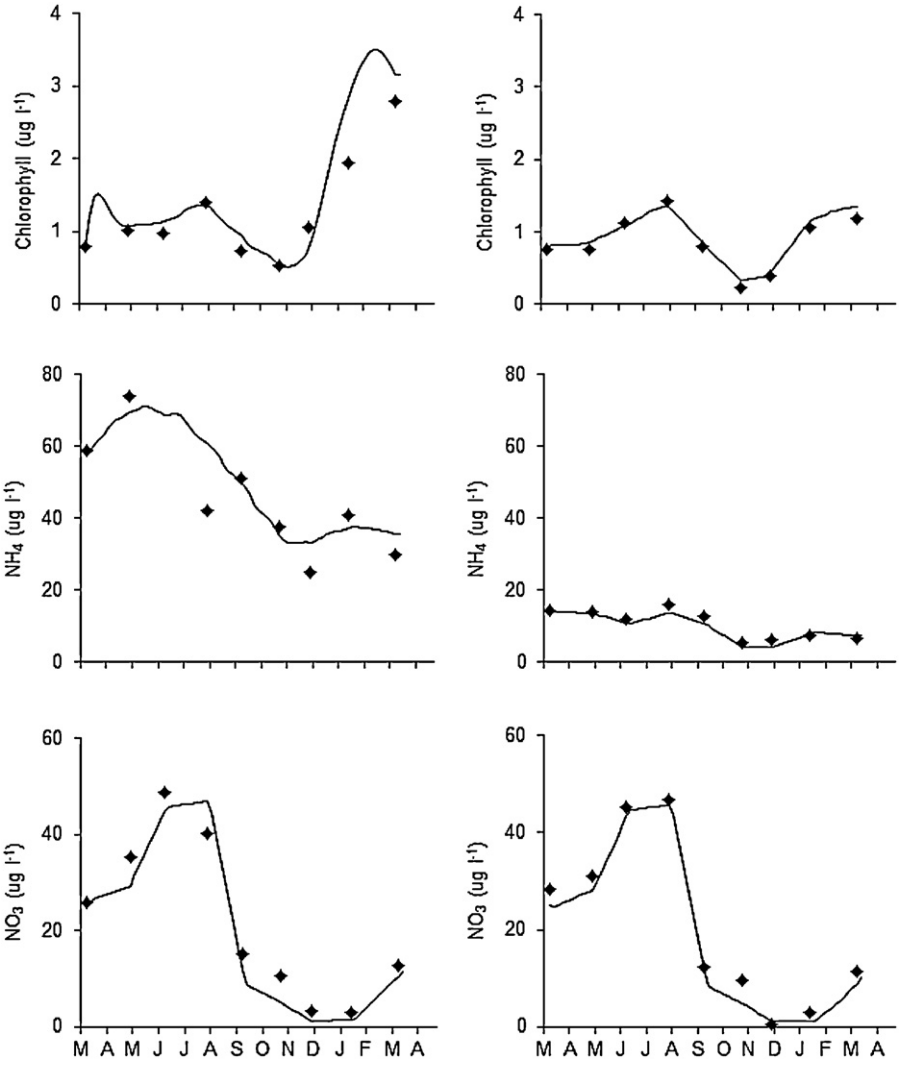


**Fig. 4.** Comparison of simulated (lines) and observed (dots) pelagic variables for current farming practice in Waihinau Bay (left column) and Port Ligar (right column) during March 2007 and April 2008.

The volume of the pelagic nutrient compartments associated with the farms was determined by continuously releasing neutrally buoyant particles from the farms. For simulating $NH_4$ dispersal, the particles were given an initial relative mass ($M_0$) of 1 with an exponential decay of the form $M(t) = M_0 \cdot exp(-k \cdot t)$ and a decay rate ($k$) of 0.1 $d^{-1}$. $NH_4$ concentrations in the bay reached 95% of steady state within ~30 days. The model was therefore run for 30 days and $NH_4$ concentrations were averaged over the next 6 tidal cycles. This provided a spatial map of average concentrations relative to the release rate. Contours were fitted to the map of average $NH_4$ contours, and the contour containing 90% of the $NH_4$ mass used to define the volume of the nutrient compartment.

After the sizes and locations of the compartments were determined, daily exchange rates of water volume between boxes were calculated using the hydrodynamic model. The model was run using the 7 largest tidal constituents as boundary conditions in order to simulate the tidal flows (Plew, 2011). The daily water volume exchanges between compartments were calculated by integrating the flow through the boundaries of each compartment.

### 3.5. Simulations of current farming practices

The model was initially set up to simulate the dynamics of both salmon and mussel monoculture systems. The simulated values of chlorophyll-*a* generally reflect the temporal variation of the observations with high biomass occurred in winter (August) and early autumn (March) (Fig. 4). The high nutrient concentrations in the salmon farm were not considered to drive phytoplankton growth during winter months in 1997. However, phytoplankton responded to high nutrient concentrations from late 1997 along with increases of both temperature and irradiance from late spring and summer. The model also responded adequately to the difference in mussel growth rates between salmon and mussel farms. High chlorophyll concentrations in the salmon farm drove the mussels to grow with significantly higher rates than in the mussel farms (Fig. 5). In addition, winter and spring were fast growth periods corresponding with high phytoplankton biomass, while slow or non-growth occurred during summer.

The simulated $NH_4$ in Port Ligar closely followed boundary conditions with high values in winter months and low values in summer (Fig. 4). Nutrient enhancement through ammonia excretion in the mussel farm was not as prominent as in the salmon farm. The ammonia level in the salmon farm was considerably higher, on average 4 times that in the mussel farm. The variation in ammonia agrees with the variation of fish biomass over the simulation period (Fig. 3). The simulated $NO_3$ in both mussel and salmon farms matched the observed values reasonably well.

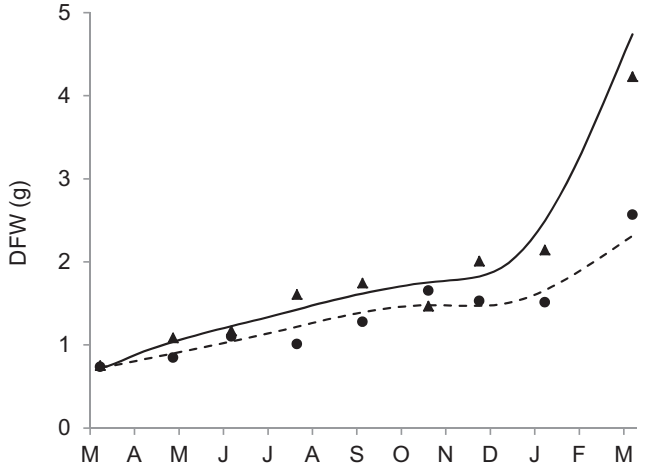


**Fig. 5.** Comparison of the observed (dots and triangles) and simulated (lines) growth of dry flesh weight of the greenshell mussel in fish and mussel farms during March 2007 and April 2008. Triangles and solid line are respectively, the observed and simulated mussel growth in the fish farm in Waihinau Bay. Dots and broken line are respectively, the observed and simulated mussel growth in the mussel farm in Port Ligar.

For the mussel farm, the simulated $NH_4$ excretion showed little variation during the period of March 2007–November 2008 (Fig. 6), despite mussel growth. This resulted from low temperatures during the period when the effect of body size on $NH_4$ excretion was offset by the effect of temperature. With increase in temperature during summer, $NH_4$ excretion increased at a considerable rate. By the end of the simulation, $NH_4$ level had increased by three times the value in November 2008. The daily $NH_4$ excretion from the salmon farm was consistent with fish biomass and considerably higher than from the mussel farm.

In the benthic sediment compartment, the model simulation indicated that daily biodeposition rates from mussel farms ranged between 0.15 and 0.50 $gC\,m^{-2}\,d^{-1}$ (Fig. 7). Despite high phytoplankton biomass in winter, the biodeposition rate under the mussel farm was low. Biodeposition rates below the salmon farm were a few hundred times higher than under mussel farms.

## 4. IMTA scenario simulations

The model simulations show conversion from monoculture to IMTA would result in considerable seaweed production over the simulation period (Fig. 8). The biomass per unit area in the salmon farm was over 100 times that in the mussel farm. At the same time, the model predicts that IMTA scenarios could result in average optimal nutrient reduction efficiencies of about 70% (Fig. 9). Overall, the nutrient reduction in the fish farm is not as efficient as in the mussel farms. Total mussel excretion is largely driven by temperature, while the fish excretion rate mainly depends on culture biomass and quality and quantity of add-in feed.

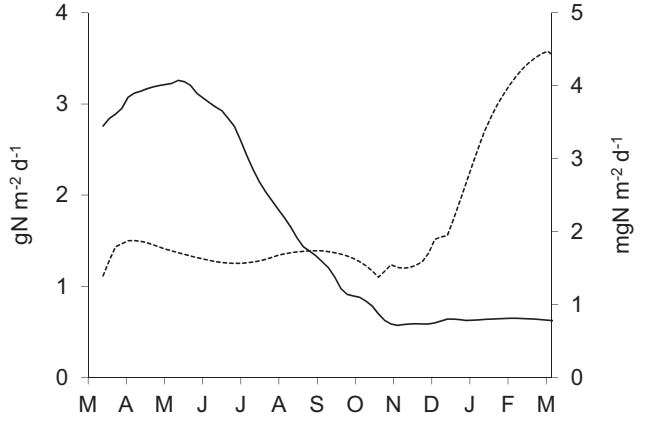


**Fig. 6.** Simulated ammonia excretion rates of the current farming practice in Waihinau Bay (solid line, left axis) and Port Ligar (dashed line, right axis) for IMTA scenarios.

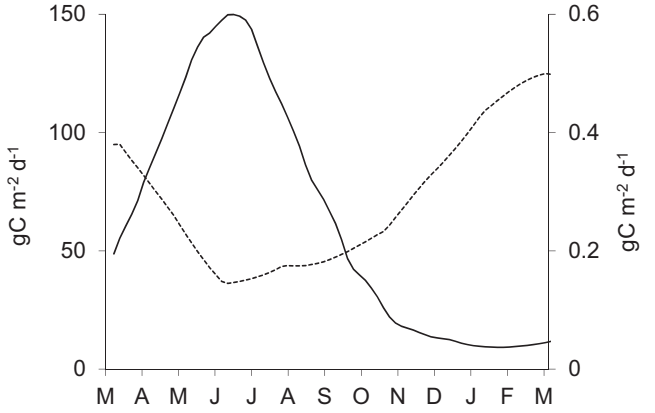


**Fig. 7.** Simulated biodeposition rates of the current farming practice from the fish farm in Waihinau Bay (solid line, left axis) and mussel farms in Port Ligar (dashed line, right axis) during March 2007 and April 2008.

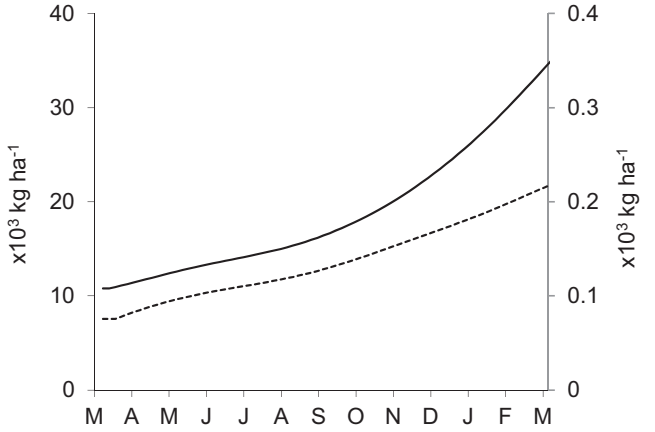


**Fig. 8.** Simulated seaweed biomass (dry weight) in Waihinau Bay (solid line, left axis) and Port Ligar (dashed line, right axis) for IMTA scenarios.

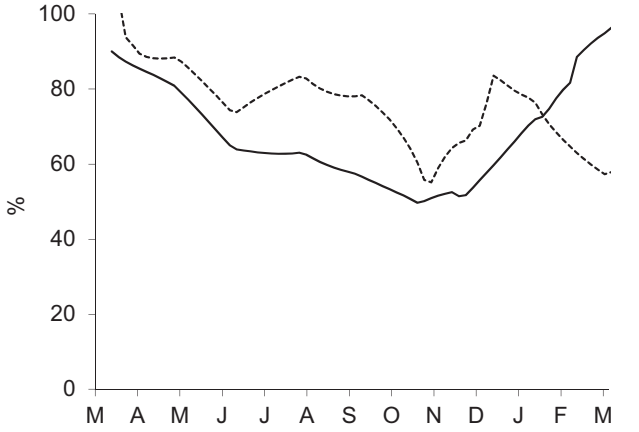


**Fig. 9.** Simulated reduction efficiency of excreted nutrients ($NH_4$) for IMTA scenarios in Waihinau Bay (solid line) and Port Ligar (dashed line).

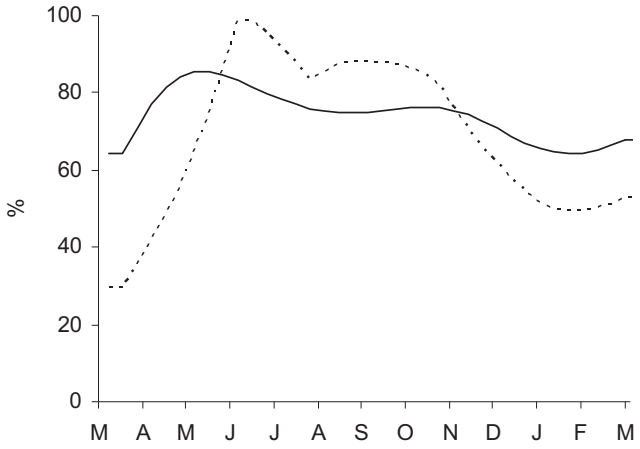


**Fig. 10.** Simulated reduction efficiency of biodeposition for IMTA scenarios in Waihinau Bay (solid line) and Port Ligar (dashed line).

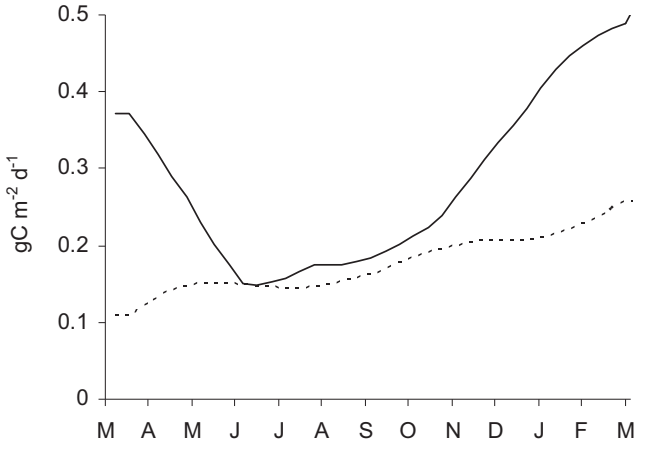


**Fig. 11.** Simulated biodeposition (solid line) and consumption by sea cucumbers (dashed line) under mussel farm in Port Ligar for IMTA scenarios.

With the co-culture of sea cucumbers, the model predicted that by the end of the simulation period, the IMTA practice could theoretically yield 210 kg ha$^{-1}$ and 25,000 kg ha$^{-1}$ biomass of sea cucumbers, respectively from the mussel and fish farms. Because biodeposition increased consistently with the growth of fish, optimising biomass of sea cucumbers is straightforward under the fish farm, ignoring at this point the constraints that relate to benthic containment (cages) and/or free ranching. However, a strong variation of biodeposition rate over the simulation period under the mussel farm makes it difficult to estimate the appropriate biomass of sea cucumbers. Based on the balance between biodeposition and consumption rates, the model predicts that optimum numbers of each cohort were 500 and 30,000 individuals per hectare, respectively under the mussel and fish farms. The simulated reduction efficiency of biodeposition is shown in Fig. 10. It is less variable under the fish farm than under the mussel farm. Potentially up to 70% of the material that settles on the seafloor could be consumed by the predicted optimal sea cucumber density. The simulated average annual growth rate of sea cucumbers across all cohorts was higher under the fish farm (260%) than under the mussel farm (180%).

## 5. Discussion

The primary motivation to develop the IMTA model was to provide a quantitative tool for the development and management of IMTA practices through mapping energetic pathways between trophic groups and their environment. Application can assist designing IMTA practices to maximise resource utilisation and minimise environmental impacts.

The feasibility of a modelling approach for general management in the aquaculture industry hinges on the flexibility of a model for various species and portability between farming systems. Because the IMTA concept is very flexible, it can be applied to open-water, land-based, marine and freshwater systems (Chopin et al., 2008) and therefore the choice of secondary organisms should be based on their commercial value as well as biomitigation potential in the local farm environment. Practically, culture feasibility, economic value and social potential are primary consideration for both principal and secondary species (see Chopin et al., 2008). Up to date, there have been different mixed-species aquaculture systems in study and in operation worldwide (Barrington et al., 2009). Through the lack of predictive modelling tools, both experimental and commercial-scale operations have been dependent on field trials and results remains semi-quantitative (see Neori et al., 2004; Chopin et al., 2008). Some effort has been made to model salmonid solid and soluble nutrient loading for co-culture trials of seaweeds and mussels in salmon farms (Angel and Freeman, 2009). The authors have recognised the need to develop flexible models that can simulate co-culture interactions and the effects of IMTA systems on water quality inside and around the farm. We believe that the present model accommodates this flexibility. The development of energetic sub-models that are specific to a trophic group is based on DEB theory that species share the commonality in physiology and hence follow the same energetic pathways across species (Kooijman, 2000). In addition, the temperature effect on the rate processes of all biological groups follows a single Arrhenius relationship. The model is transferable to other IMTA systems with species combination of finfish–shellfish-detritivore-primary producer for optimising yields and reducing farm-derived wastes. Adjustments lie in the parameterisation for local environmental processes and hydrodynamic properties.

The capability of the model has been examined through IMTA scenario simulations for both fish and mussel farms where crop species of different cohorts were all seeded at the same time. Although this assumption was somewhat arbitrary, the model outputs have helped us understand system behaviours of the IMTA scenarios. Generally, the model could generate reasonable outcomes on the required biomass of each trophic level for the prescribed IMTA system. The model outcomes have shown that IMTA practices would considerably reduce environmental impacts. Simulations have also illustrated some of the difficulties in optimising production and bioremediation on an IMTA farm. One of the important features is that the consumption rate of sea cucumbers mismatched the mussel biodeposition rate during the simulation period, particularly during the first few months of the simulation (Fig. 11). The biodeposition rate showed clear seasonal variation, while the sea cucumber consumption generally showed an increasing trend. This mismatch resulted from the difference in physiological characteristics: mussel biodeposition rate depends on food supplies and temperature (e.g. Hawkins et al., 1999), while the consumption of sea cucumber is largely affected by temperature (e.g. Yang et al., 2005). Although the biomass of sea cucumbers could be increased to match mussel biodeposition rate initially, this would cause less food availability and starvation during some periods, particularly in winter months when biodeposition rate is low. This disagreement between consumption and biodeposition would cause low reduction efficiency where a large fraction of the biodeposition remains in the system. The optimisation between consumption and biodeposition rates could be achieved through manipulations of stocking density, seeding time and harvesting frequencies, but any proposals for culture operations should be

economically practicable and cost-effective. Therefore, acceptable levels of reduction efficiency would account for feasibility and profitability of culture operations. For the salmon farm, however, the biodepostion rate matched reasonably well with the consumption rate of sea cucumbers, reflecting little variation of reduction efficiency (Fig. 10). This result is very promising for the development of fish-based IMTA practices, as it is feasible to achieve acceptable levels of consumption rate and reduction efficiency without additional costs resulting from multiple stocking density and harvesting operations. Because finfish aquaculture can cause much higher environmental impacts than shellfish farming (see Hatcher et al., 1994; Buschmann et al., 2006), the co-culture of sea cucumbers would have promising mitigation potential.

Development of the novel IMTA model is not without difficulties and shortcomings. Some knowledge gaps have been detected, one of which is the lack of comprehensive physiological information for potential co-culture species in New Zealand. Although this would have contributed some uncertainties in the parameterisation of the DEB sub-models, model simulations may not have been greatly compromised. The variation of parameter values may not be considerable between related functional species and hence borrowing parameter values is common in bioenergetic modelling studies. For example, a model for sockeye salmon could successfully predict the behaviour of coho salmon and chinook salmon (e.g. Stewart and Ibarra, 1991). Similarly, other studies have shown that rainbow trout metabolism was an adequate substitute for chinook salmon metabolism (Madenjian et al., 2004). In addition, some limited information indicates that physiological rates of sea cucumber (*A. mollis*) are similar to those of *S. japonicus* and the rates of seaweed (*E. radiata*) are close to the parameter values used in the model (NIWA unpubl. data). Nonetheless, the model has contributed to understanding the dynamics of IMTA systems and provided a quantitative tool for designing and managing IMTA practices. Our approach to development an IMTA model is juxtaposed with field experimentations. The identified knowledge gaps will direct future experimentations.

In conclusion, the development of IMTA practices, the balanced ecosystem approach, is bound to play a major role worldwide in sustainable expansions of aquaculture (Soto, 2009). An IMTA ecosystem model is a useful tool for gauging optimal stocking scenarios based on the predicted amounts of farm-derived wastes. The model structure is flexible for application to different IMTA operations. Further improvement of the model would rely on comprehensive physiological information of trophic species collected from specially designed experiments that provide data suitable for modelling requirements. The predictive accuracy of the model presented here will be enhanced with feedback from monitored commercial IMTA farms that are likely to grow in number as pressure for space increases and environmental accountable becomes more acute across the world.

## Acknowledgements

We gratefully acknowledge two anonymous reviewers for their critical comments. This study was supported by the New Zealand Foundation of Research, Science and Technology, Contract Number C01X0513, with international investment opportunity fund in collaboration with Yellow Sea Fisheries Research Institute in China.

## References

Alfaro, A.C., 2001. Ecological dynamics of the greenshell-lipped mussel, *Perna canaliculus*, at Ninety Mile Beach, Northern New Zealand. Ph.D. Thesis. Univ Auckland, New Zealand.

Amundsen, P.A., Bergersen, R., Huru, H., Heggberget, T.G., 1999. Diel feeding rhythms and daily food consumption of juvenile Atlantic salmon in the River Alta, northern Norway. Journal of Fish Biology 54, 58–71.

Andersen, V., Nival, P., 1987. Modelling of planktonic ecosystem in an enclosed water column. Journal of the Marine Biological Association of the United Kingdom 67, 407–430.

Angel, D., Freeman, S., 2009. Integrated aquaculture (INTAQ) as a tool for an ecosystem approach in the Mediterranean Sea. In: Soto, D. (Ed.), Integrated Mariculture: A Global Review. FAO Fisheries and Aquaculture Technical Paper 529, Rome, pp. 133–183.

Bacher, C., Duarte, P., Ferreira, J.G., Héral, M., Raillard, O., 1998. Assessment and comparison of Marennes-Oléron Bay (France) and Carlingford Lough (Ireland) carrying capacity with ecosystem models. Aquatic Ecology 31, 379–394.

Barrington, K., Chopin, T., Robinson, S., 2009. Integrated multi-trophic aquaculture (IMTA) in marine temperate waters. In: Soto, D. (Ed.), Integrated Mariculture: A Global Review. FAO Fisheries and Aquaculture Technical Paper 529, Rome, pp. 7–46.

Beauchamp, D.A., Cross, A.D., Armstrong, J.L., Myers, K.W., Moss, J.H., Boldt, J.L., Haldorson, L.J., 2007. Bioenergetic responses by Pacific salmon to climate and ecosystem variation. North Pacific Anadromous Fish Commission Bulletin 4, 257–269.

Bienfang, P.K., 1977. A new phytoplankton sinking rate method suitable for field use. Deep-Sea Research I 26, 719–729.

Buschmann, A.H., Riquelme, V.A., Hernández-González, M., Varela, D., Jiménez, J.E., Henríquez, L.A., Vergara, P.A., Guíñez, R., Filún, a.L., 2006. A review of the impacts of salmonid farming on marine coastal ecosystems in the southeast Pacific. Journal of Marine Science 63, 1338–1345.

Buschmann, A.H., Varela, D.A., Hernández-González, M.C., Huovinen, P., 2008. Opportunities and challenges for the development of an integrated seaweed-based aquaculture activity in Chile: Determining the physiological capabilities of *Macrocystis* and *Gracilaria* as biofilters. Journal of Applied Phycology 20, 571–577.

Caperon, J., Meyer, J., 1972. Nutogeon limited growth of marine phytoplankton. II. Uptake kinetics and their role in nutrient limited growth of phytoplankton. Deep-Sea Research 19, 619–632.

Chapelle, A., Lazure, P., Ménesguen, A., 1994. Modelling eutrophication events in a coastal ecosystem. Sensitivity analysis. Estuarine and Coastal Marine Science 39, 529–548.

Chapelle, A., 1995. A preliminary model of nutrient cycling in sediments of a Mediterranean lagoon. Ecological Modelling 80, 131–147.

Chopin, T., Robinson, S.M.C., Troell, M., Neori, A., Fang, J., 2008. Multitrophic integration for sustainable marine aquaculture. In: Jørgensen, S.E., Fath, B.D. (Eds.), The Encyclopedia of Ecology, Ecological Engineering, vol. 3. Elsevier, Oxford, pp. 2463–2475.

Chopin, T., Robinson, S., Sawhney, M., Bastarache, S., Belyea, E., Shea, R., Armstrong, R., Stewart, I., Fitzgerald, P., 2004. The AquaNet integrated multi-trophic aquaculture project: rationale of the project and development of kelp cultivation as the in organic extractive component of the system. In: Proceedings of the Integrated Multi-Trophic Aquaculture Workshop, p. 11.

Corkett, C.J., Maclaren, I.A., 1979. The biology of *Pseudocalanus*. Advances in Marine Biology 15, 2–231.

Devola, A.H., Uhlenhopp, A.G., Naqvi, S.W.A., Brandes, J.A., Jayakumar, D.A., Naik, H., Gaurin, S., Codispoti, L.A., Yoshinari, T., 2006. Denitrification rates and excess nitrogen gas concentrations in the Arabian Sea oxygen deficient zone. Deep-Sea Research I 53, 1533–1547.

Dowd, M., 2005. A bio-physical coastal ecosystem model for assessing environmental effects of marine bivalve aquaculture. Ecological Modelling 183, 323–346.

Duarte, P., Ferreira, J.G., 1993. A methodology for parameter estimation in seaweed productivity modelling. Hydrobiologia 260–261, 183–189.

Duarte, P., Meneses, R., Hawkins, A.J.S., Zhu, M., Fang, J., Grant, J., 2003. Mathematical modelling to assess the carrying capacity for multi-species culture within coastal waters. Ecological Modelling 168, 109–143.

Dutkiewicz, S., Follows, M., Marshall, J., Gregg, W.W., 2001. Interannual variability of phytoplankton abundances in the North Atlantic. Deep-Sea Research II 48, 2323–2344.

Edwards, A., Grantham, B.E., 1986. Inorganic nutrient regeneration in Loch Etive bottom water. In: Skreslet, S. (Ed.), The Role of Freshwater Outflow in Coastal Marine Ecosystems. Springer-Verlag, Berlin, pp. 195–204.

Finstad, A.G., Ugedal, O., Forseth, T., Næsje, T.F., 2004. Energy-related juvenile winter mortality in a northern population of Atlantic salmon (*Salmo salar*). Canadian Journal of Fisheries and Aquatic Sciences 61, 2358–2368.

Fralick, R.A., Baldwin, H.P., Neto, A.I., Hehre, E.J., 1990. Physiological responses of *Pterocladia* and *Gelidium* (Gelidiales Rhodophyta) from the Azores. Portugal Hydrobiologia 204–205, 479–482.

Fransz, H.G., Mommaerts, J.-P., Radach, G., 1991. Ecological modelling of the North Sea. Netherlands Journal of Sea Research 28, 67–140.

Gibbs, M.M., Vant, W.N., 1997. Seasonal change in factors controlling phytoplankton growth in Beatrix Bay, New Zealand. New Zealand Journal of Marine and Freshwater Research 31, 237–248.

Goldman, J.C., 1977. Temperature effects on phytoplankton growth in continuous culture. Limnology and Oceanography, 932–935.

Grangeré, K., Lefebvre, S., Bacher, C., Cugier, P., Ménesguen, A., 2010. Modelling the spatial heterogeneity of ecological processes in an intertidal estuarine bay: dynamic interactions between bivalves and phytoplankton. Marine Ecology Progress Series 415, 141–158.

Grant, J., Curran, K.J., Guyondet, T.L., Tita, G., Bacher, C., Koutitonsky, V., Dowd, M., 2007. A box model of carrying capacity for suspended mussel aquaculture in Lagune de la Grande-Entrée. Iles-de-la-Madeleine, Québec. Ecological Modelling 200, 193–206.

Graynoth, E., 1995. Spawning migrations and reproduction of landlocked sockeye salmon (*Oncorhynchus nerka*) in the Waitaki catchment, New Zealand. New Zealand Journal of Marine & Freshwater Research 29, 257–269.
Hatcher, J., Grant, J., Schofield, B., 1994. Effects of suspended mussel culture (*Mytilus* spp.) on sedimentation benthic respiration and sediment nutrient dynamics in a coastal bay. Marine Ecology Progress Series 115, 219–235.
Hawkins, A.J.S., James, M.R., Hickman, R.W., Hatton, S., Weatherhead, M., 1999. Modelling of suspension-feeding and growth in the green-lipped mussel *Perna canaliculus* exposed to natural and experimental variations of seston availability in the Marlbourough Sounds, New Zealand. Marine Ecology Progress Series 191, 217–232.
Hickman, R.W., 1979. Allometry and growth of the green-lipped mussel *Perna canaliculus* in New Zealand. Marine Biology 51, 311–327.
Hughes A.D., Kelly, M.S., 2011. Integrated Multi-Trophic Aquaculture. Scottish Association of Marine Science, 15 p. http://www.sarf.org.uk/cms-assets/documents/28926-823833.current-state-of-integrated-aquaculture.
Kiefer, D.A., 1990. A reply to the comment by Bannister. Limnology and Oceanography 35, 980–982.
Kiørboe, T., Møhlenberg, F., Hamburger, K., 1985. Bioenergetics of the copepod *Acartia tonsa*: relation between feeding, egg production and respiration, and composition of specific dynamic action. Marine Ecology Progress Series 26, 85–97.
Kleiber, M., 1961. The Fire of Life: An Introduction to Animal Energetics. Wiley, New York.
Kooijman, S.A.L.M., 2000. Dynamic Energy and Mass Budgets in Biological Systems. Cambridge University Press, Cambridge.
Li, S., Zhang, G., Wang, B., 1983. Coculture of kelp (*Laminaria haponicus* Aresch) and scallop (Chlamys farreri Jones et Preston). Transactions of Oceanology and Limnology 4, 70–75.
Madenjian, C.P., O'Connor, D.V., Chernyak, S.M., Rediske, R.R., O'Keefe, J.P., 2004. Evaluation of a chinook salmon (*Oncorhynchus tshawytscha*) bioenergetics model. Canadian Bulletin of Fisheries and Aquatic Sciences 61, 627–635.
Mao, X., Zhu, M., Yang, X., 1993. The photosynthesis and productivity of benthic macrophytes in Sanggou Bay. Acta Ecologica Sinica. 13, 25–29.
Marsden, I.D., Weatherhead, M.A., 1999. Short-level induced variations in condition and feeding of the mussel *Perna canaliculus* from the east coast of the South Island, New Zealand. New Zealand Journal of Marine and Freshwater Research 33, 611–622.
Møller, L.F., Riisgård, H.U., 2007. Respiration in the scyphozoan jellyfish Aurelia aurita and two hydromedusae (*Sarsia tubulosa* and *Aequorea vitrina*): effect of size, temperature and growth. Marine Ecology Progress Series 330, 149–154.
Munch, S.B., Conover, D.O., 2002. Accounting for local physiological adaptation in bioenergetic models: testing hypotheses for growth rate evolution by virtual transplant experiments. Canadian Journal of Fisheries and Aquatic Sciences 59, 393–403.
NACA, 1989. Integrated Fish Farming in China. FAO NACA Technical Manual 7. A World Food Day Publication of the Network of Aquaculture Centres in Asia and the Pacific, Bangkok, Thailand, 278 pp.
Nakata, K., Horiguchi, F., Yamamuro, M., 2000. Model study of Lake Shinji and Nakaumi – a coupled coastal lagoon system. Journal of Marine Systems 26, 145–169.
Neori, A., Chopin, T., Troell, M., Buschmann, A.H., Kraemer, G.P., Halling, C., Shpigel, M., Yarish, C., 2004. Integrated aquaculture: rationale, evolution and state of the art emphasizing seaweed biofiltration in modern mariculture. Aquaculture 231, 361–391.
Piedecausa, M.A., Aguado-Giménez, F., García-García, B., Ballester, G., Telfer, T., 2009. Settling velocity and total ammonia nitrogen leaching from commercial feed and faecal pellets of gilthead seabream (*Sparus aurata* L. 1758) and seabass (*Dicentrarchus labrax* L. 1758). Aquaculture Research 40, 1703–1714.
Plew, D.R., 2011. Shellfish farm-induced changes to tidal circulation in an embayment and implications for seston depletion. Aquaculture Environment Interactions 1, 201–214.
Pouvreau, S., Bourles, Y., Lefebvre, S., Gangnery, A., Alunno-Bruscia, M., 2006. Application of a dynamic energy budget model to the Pacific oyster, *Crassostrea gigas*, reared under various environmental conditions. Journal of Sea Research 56, 156–167.
Pujo-Pay, M., Conan, P., Raimbault, P., 1997. Excretion of dissolved organic nitrogen by phytoplankton assessed by wet oxidation and $^{15}N$ tracer procedures. Marine Ecology Progress Series 153, 99–111.
Reeve, M.R., 1980. Comparative experimental studies on the feeding of chaetognaths and ctenophores. Journal of Plankton Research 2, 381–393.
Reid, G.K., Liutkus, M., Robinson, S.M.C., Chopin, T.R., Blair, T., Lander, T., Mullen, J., Page, F., Moccia, R.D., 2009. A review of the biophysical properties of salmonid faeces: implications for aquaculture waste dispersal models and integrated multi-trophic aquaculture. Aquaculture and Research 40, 257–273.
Ren, J.S., Ross, A.H., 2005. Environmental influence on mussel growth: A dynamic energy budget model and its application to the greenshell mussel *Perna canaliculus*. Ecological Modelling 189, 347–362.
Ren, J.S., Ross, A.H., Hadfield, M.G., Hayden, B.J., 2010. An ecosystem model for estimating potential shellfish culture production in sheltered coastal waters. Ecological Modelling 221, 527–539.
Ross, A.H., Gurney, W.S.C., Heath, M.R., Hay, S.J., Henderson, E.W., 1993. A strategic simulation model of a fjord ecosystem. Limnology and Oceanography 38, 128–153.
Smaal, A.C., Vonck, A.P.M.A., 1997. Seasonal variation in C, N and P budgets and tissue composition of the mussel *Mytilus edulis*. Marine Ecology Progress Series 153, 167–179.
Soto, D., 2009. Integrated Mariculture: A Global Review. FAO Fisheries and Aquaculture Technical Paper 529, Rome, 183 pp.
Soto, D., Jara, F., 2007. Using natural ecosystem services to diminish salmon-farming footprints in Southern Chile. In: Bert, T.M. (Ed.), Ecological and Genetic Implications of Aquaculture Activities. Springer, Netherlands, pp. 459–475.
Stead, S.M., Houlihan, D.F., McLay, H.A., Johnstone, R., 1999. Food consumption and growth in maturing Atlantic salmon (*Salmo salar*). Canadian Journal of Fisheries and Aquatic Sciences 56, 2019–2028.
Stevens, E.D., Sutterlin, A., Cook, T., 1998. Respiratory metabolism and swimming performance in growth hormone transgenic Atlantic salmon. Canadian Journal of Fisheries and Aquatic Sciences 55, 2028–2035.
Stewart, D.J., Ibarra, M., 1991. Predation and production by salmonine fishes in Lake Michigan 1978–88. Canadian Journal of Fisheries and Aquatic Sciences 48, 902–922.
Taylor, M.W., Rees, T.A.V., 1999. Kinetics of ammonium assimilation in two seaweeds *Enteromorpha* sp. (chlorophyceae) and *Osmundaria colensoi* (rhodophyceae). Marine Ecology Progress Series 35, 740–764.
Tett, P., Droop, M.R., 1988. Cell quota models and planktonic primary production. In: Wimpenny, J.W.T. (Ed.), Handbook of Laboratory Model Systems for Microbial Ecosystems, vol. 2. CRC Press, Boca Raton, pp. 77–233.
Tyler, I.D., 1983. A carbon budget for Creran a Scottish sea-loch. Ph.D. Thesis. Univ Strathclyde.
van der Veer, H.W., Cardoso, J.F.M.F., van der Meer, J., 2006. The estimation of DEB parameters for various North Atlantic bivalve species. Journal of Sea Research 56, 107–124.
van der Meer, J., 2006. An introduction to dynamic energy budget (DEB) models with species emphasis on parameter estimation. Journal of Sea Research 56, 85–102.
Wang, D., 2001. Development and application of shellfish aquaculture technology. Journal of Oceanography of Huanghai and Bohai Seas 19, 78–81.
Widmer, C.L., 2005. Effects of temperature on growth of north-east Pacific moon jellyfish ephyrae, *Aurelia labiata* (Cnidaria: Scyphozoa). Journal of the Marine Biological Association of the United Kingdom 85, 569–573.
Yang, H., Wang, J., Zhou, Y., Zhang, T., Wang, P., He, Y., Zhang, F., 2000. Comparison of efficiencies of different culture systems in the shallow sea along Yantai. Journal of Fishery Sciences of China 24, 140–145.
Yang, H., Yuan, X., Zhou, Y., Mao, Y., Zhang, T., Liu, Y., 2005. Effects of body size and water temperature on food consumption and growth in the sea cucumber *Apostichopus japonicus* (Selenka) with special reference to aestivation. Aquaculture Research 36, 1085–1092.
Yurista, P.M., 1999. A model for temperature correction of size-specific respiration in *Bythotrephes cederstroemi* and *Daphnia middendorffiana*. Journal of Plankton Research 21, 721–734.
Zlotnik, I., Dubinsky, Z., 1989. The effect of light and temperature on DOC excretion by phytoplankton. Limnology and Oceanography 34, 831–839.